Electronic Supplementary Information

An electrochemical sensor based on enzyme-free recycling amplification for sensitive and specific detection of miRNAs from cancer cells

Lili Jiang[a], Yuling Yang[a], Yuhong Lin[a], Ziyi Chen[a], Chao Xing[a], Chunhua Lu[a]*, Huanghao Yang[a] and Shusheng Zhang[b]*

[a] MOE Key Laboratory for Analytical Science of Food Safety and Biology, Fujian Provincial Key Laboratory of Analysis and Detection Technology for Food Safety, State Key Laboratory of Photocatalysis on Energy and Environment, College of Chemistry, Fuzhou University, Fuzhou 350108, P.R. China

[b] Collaborative Innovation Center of Tumor Marker Detection Technology, Equipment and Diagnosis-Therapy Integration in Universities of Shandong, College of Chemistry and Chemical Engineering, Linyi University, Linyi 276005, P.R. China

Corresponding author. Tel.: +86-591-22866135
E-mail address: chunhualu@fzu.edu.cn shushzhang@126.com

Experimental section

Materials and Reagents

All miRNA and DNA sequences were synthesized from Sangon Biotechnology Company, Ltd. (Table S1). Tris(2-carboxyethy) phosphine hydrochloride (TCEP) and 6- Mercaptohexanol (MCH) supplied by Sigma (St. Louis, MO, USA). All solutions were prepared with ultrapure water (Milli-Q, 18 MΩ·cm resistivity at 25 °C, Merck Millipore) without further purification.

Cell Culture and extraction of total RNA from cells

The human breast cancer cells (MCF-7) and human cervical cancer cells (HeLa) were elaborately cultured in RPMI 1640 medium (Hyclone), which was supplemented with 10 % fetal bovine serum (FBS, Hyclone) and 100 IU/mL penicillin-streptomycin in humidified chamber containing 5% CO_2 at 37 °C. The RNA samples were obtained from Hela and MCF-7 cells through the ExCellenCT Lysis Kit by following the manufacturer's proposed protocol.

Non-denaturing polyacrylamide gel electrophoresis (PAGE)

The samples were mixed with the DNA-loading buffer (volume ratio 5:1), and then examined by polyacrylamide-gel electrophoresis (PAGE) on a freshly prepared 16 % polyacrylamide gel in 1 × TBE buffer at 100 V for 60 min. Polyacrylamide-gel electrophoresis (PAGE) was conducted with a Bio-Rad imaging system (Hercules, CA).

Electrochemical Measurements

Electrochemical measurements were carried out with a CHI 660D workstation (CH Instruments Inc., Shanghai, China) using a conventional three-electrode configuration that consisted of the platinum wire auxiliary electrode, the Ag/AgCl reference electrode and the working AuE (2 mm in diameter). Square wave voltammetry (SWV) was performed in PBS (10 mM) with a step potential of 4 mV, a frequency of 25 Hz, and an amplitude of 25 mV. The electrochemical impedance spectroscopy (EIS) experiments were performed using 20 mM $[Fe(CN)_6]^{3-/4-}$ containing 1 M KCl with a frequency ranging from 1 to 10^5 Hz and amplitude set at 5 mV.

Table S1. Sequences of the oligonucleotides (in 5' to 3'direction)

Oligonucleotide	Sequence (from 5′ to 3′)
H0	AGT GTC ACG TTC CTG TGT TGA CTC AAC ATC AGT CTG ATA AGC TAA GTC AAC ACA GGA
H0-141	AGT GTC ACG TTC CTG TGT TGA CCC ATC TTT ACC AGA CAG TGT TAC GTC AAC ACA GGA
H1	GTC AA CAG AGG AAC GTG ACA CTC ATG GAT GCT CAG TGT CAC GTT CCT
H2	TGA CAC TGA GCA TCC ATG AGT GTC ACG TTC CTC ATG GAT GCT CGT C
L	GAC GAG CAT CCA TGG TGT TGA C
S-MB	GTC AAC ACC ATG GAT-MB
S	GTC AAC ACC ATG GAT
CP	SH-(CH2)6-CAC ATC ATC CAT GGT GTT
MiRNA-21	UAG CUU AUC AGA CUG AUG UUG A
MiRNA-141	UAA CAC UGU CUG GUA AAG AUG G
MiRNA-21(1)	UAG CUU AUC A**A**A CUG AUG UUG A
MiRNA-21(3)	U**C**G CUU AUC **G**GA CUG AU**C** UUG A

Table S2. Comparison of different methods for the detection of miRNA

method	strategy	Linear range	LOD	Ref
Fluorescence	Catalytic hairpin assembly and enzymatic repairing amplification	100 fM -100 nM	50 fM	38
Fluorescence	An ATP-fueled nucleic acid signal amplification	50 pM - 10nM	18pM	39
Fluorescence	Magnetic microbead-assisted catalyzed hairpin assembly	0.1 nM - 4 nM	34 pM	40
SERS	Multicolor Gold-Silver Nano-Mushrooms	10 fM - 100 pM.	10 fM	41
Electrochemistry	Exonuclease-III-assisted target recycling amplification and mismatched catalytic hairpin assembly	100 fM - 5 nM	92 fM	42
Electrochemistry	Exonuclease-assisted target recycling	0.01 pM - 100 pM	3.5 fM	43
Electrochemistry	sandwich assay onto magnetic microcarriers and hybridization chain reaction amplification	0.2 nM - 5.0 nM	60 pM	44
Electrochemistry	A Zinc finger protein specific to DNA−RNA hybrids	2 fM -1 nM	2 fM	45
Electrochemistry	Dendritic DNA/PNA assembly	0.1 pM - 10 nM	100 fM	46
Electrochemistry	A triple-helix molecular switch	0.5 pM - 80 pM	0.12 pM	47
Electrochemistry	Catalytic hairpin assembly and DNA three-way junction	10 fM-10 nM	3.6 fM /4.5 fM	This work

Detection of miRNA in the serum-containing environment

To further investigate the application of this proposed method for real sample analysis, the target miRNA-21 was detected in human serum samples using a standard addition method. With this purpose, three different concentrations of miRNA (10, 100 and 1000 pM) were added to the 10-fold diluted healthy human serum samples and measured using the fabricated biosensor. As shown in Table S3, the recovery values and RSD for the test samples were in the range of 97.2-104.5% and 2.8-5.3%, respectively. These results clearly indicate that the fabricated biosensor has promising application for detecting diverse miRNAs in complex samples.

Table S3. Detection of miRNA-21 in human serum samples (n=5).

Sample	Added (pM)	Found (pM)	Recovery (%)	RSD (%)
1	10	10.5	105	5.3
2	100	97.2	97.2	2.8
3	1000	1045	104.5	3.9

Mean value of five parallel determination in the optimal experiment conditions.

Characterization of proposed biosensor strategy by PAGE

The detail PAGE image was shown in Fig. S1. The target miRNA-21, H0, H1, H2, CP, S, L were corresponded to the bands from lane 1 to lane 4, lane 16 to lane 18, respectively. The mixture of T and H0 showed new band (lane 5) at different from the miRNA-21and H0 (lane 1, 2), which resulted from the hybridization of H0 with miRNA-21 (T/H0 complexes). T/H0 complexes can exist as a trigger for CHA reactions. No new band appeared in the mixture of H0, H1 and H2 in the absence of target miRNA (lane 8), indicating that all hairpin reactants were stable and without false hybridizations. Upon the addition of target miRNA, a new band of high molecular weight appeared (lane 9), which was indicative of the formation of the H1/H2 complex. As expected, CHA was triggered by the T/H0 duplex. Lanes 9–18 show the formation of the DNA TWJ and the capturing capability of the CP strand. When the three hairpins (H0, H1 and H2), L/S and CP were incubated with target miRNA, the bands of H1/H2, L/S and CP attenuated with the appearance of larger molecular weight product band (DNA TWJ) and a new band corresponding to the S/CP complex (lane 12). This phenomenon was due to the hybridization of L with the H1/H2 complex to form the stable DNA TWJ complex, and the separation of S from the L/S duplex reacted with CP. No new band was observed in the presence of miRNA-21 (lane 11). While the control experiments in lane 6, 7, 9, 10, 13, 14 and 15 showed the hybridization conditions of other DNA combinations, further proved that target played a critical role in accomplishment of CHA- DWJ system. Taken collectively, these results show that the formation of the DNA TWJ was specific for target-induced assembly, and the CHA-DNA TWJ strategy was highly specific for miRNA detection.

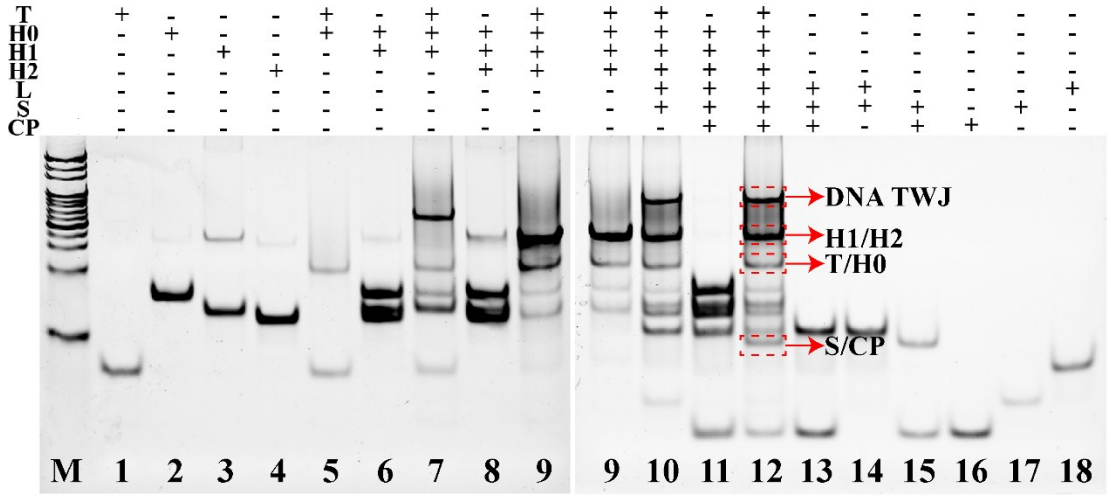

Fig. S1. The PAGE characterization of CHA and the DNA TWJ strategy.

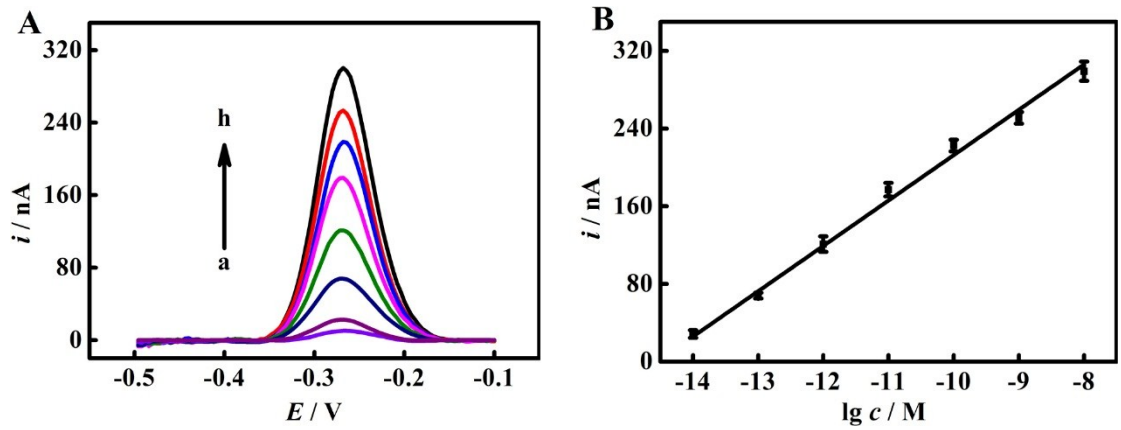

Fig. S2. (A) SWV current responses of the present biosensor to different concentrations of miRNA-141(from a to g: 0, 10 fM, 100 fM, 1 pM, 10 pM, 100 pM, 1 nM and 10 nM), (B) Calibration plot of the SWV peak current versus the logarithm of the miRNA-141 concentration. Error bars: SD; n = 3.

Reference

38 C. Zhang, Y. Tang, Y. Sheng, H. Wang, Z. Wu, J. Jiang, *Chem. Commun*., 2016, **52,** 13584-13587.

39 Z. Wen, W. Liang, Y. Zhuo, C. Xiong, Y. Zheng, R. Yuan , Y. Chai, *Chem. Commun.,* 2018,**54,**10897-10900.

40 H. Fang, N. Xie, M. Ou, J. Huang, W. Li, Q. Wang, J. Liu, X. Yang , K. Wang, *Anal. Chem.*, 2018,**90,** 7164-7170.

41 J. Su, D. Wang, L. Norbel, J. Shen, Z. Zhao, Y. Dou, T. Peng, J. Shi, S. Mathur, C. Fan ,S. Song, *Anal. Chem.*, 2017, **89,** 2531-2538

42 Campuzano, S., R. M. Torrente-Rodriguez, E. Lopez-Hernandez, F. Conzuelo, R. Granados, J.M. Sanchez-Puelles ,J. M. Pingarron, *Angew. Chem. Int. Ed.*, 2014,**53,** 6168-6171.

43 Z. Chen, Y. Xie, W. Huang, C. Qin, A. Yu ,G. Lai, *Nanoscale*,2019,**11,** 11262-11269

44 Torrente-Rodriguez, R. M., S. Campuzano, V. R. Montiel, J. J. Montoya ,J. M. Pingarron, *Biosens. Bioelectron.*, 2016,**86,** 516-521

45 C.Fang, K. Kim, B. Yu, S. Jon, M. S. Kim, H. Yang , *Anal. Chem.,* 2017,**89,** 2024-2031.

46 F. Xuan, T. W. Fan ,I. M. Hsing, ACS Nano, 2015,**9,** 5027-5033.

47 E. Xu, Z. Li, X. Zhang, J. Zhou, X. Yan, Y. Liu , J. Chen, *Anal. Chem.*, 2017,**89**, 8830−8835.